5

Forward Projection through Voxel Volumes

Forward projection through voxel volumes is a major step in all iterative reconstruction methods. In the work of this thesis we have used forward projection when generating synthetic projections of the voxelized head phantom defined in Appendix B.3.

Most of the material in this chapter, apart from Section 5.3, is based on the presentation by Köhler, Turbell, and Grass (2000). Additional experiments have also been designed in collaboration with Thomas Köhler.

5.1 Methods

We present four different approaches to forward projection. All of these methods can be classified as ray-driven, in the sense that they traverse each ray through the voxel volume while accumulating the line-integration value. Alternative approaches are discussed in Section 5.3.

5.1.1 Siddon's Method

Figure 5.1(a) shows a three-dimensional voxel grid along one axis. The sample points are centred in the voxels. If nearest-neighbour interpolation is used, the line-integral can be easily calculated as a weighted sum of the values of the intersected voxels. The weights in the sum are naturally the length of intersection between each voxel and the ray. Siddon (1985) formulated an efficient way of

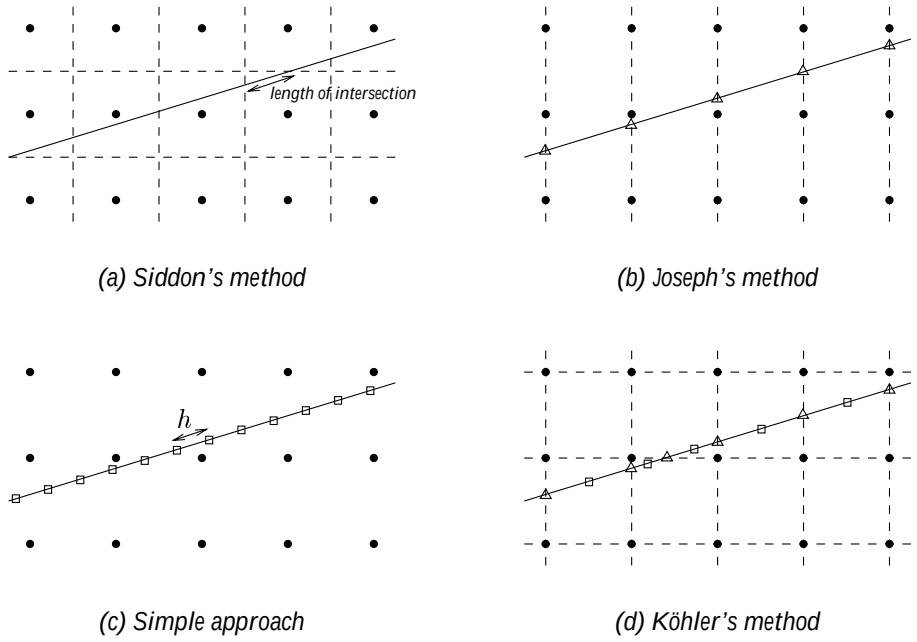

(a) Siddon's method (b) Joseph's method

(c) Simple approach (d) Köhler's method

Figure 5.1 *Four methods of line-integration as seen along one axis. Triangles indicate bi-linear interpolation, squares indicate tri-linear interpolation.*

calculating this length while traversing the ray. Other efficient ways of incrementally stepping through voxel volumes have been developed for use in computer graphics, see Cohen (1994) for further references.

The nearest neighbour interpolation is a too simplified model for most applications. Goertzen, Beekman, and Cherry (2000) present CT reconstruction experiments from data obtained using Siddon's method. They draw the conclusion that the input voxel volume has to be of at least the double resolution in each dimension compared to the desired resolution of the reconstruction.

5.1.2 Joseph's Method

Joseph (1982) describes a somewhat more elaborate forward projection method for the two-dimensional case. It is easily extended to three dimensions. Assume that the integral of the line segment between (x_1, y_1, z_1) and (x_2, y_2, z_2) is to be computed. By comparing $|x_1 - x_2|$, $|y_1 - y_2|$, and $|z_1 - z_2|$, the principal direction of the ray is first determined. We will now discuss the case where the principal direction is along the x-axis, i.e. when $|x_1 - x_2|$ is the largest of the three absolute differences. The other cases are handled in similar ways.

Figure 5.1(b) shows how a bi-linear interpolation is performed on the intersection points of each (y, z)-plane of the sampling grid. The sum of these interpolations is finally weighted with the factor

$$\frac{\sqrt{(x_1 - x_2)^2 + (y_1 - y_2)^2 + (z_1 - z_2)^2}}{|x_1 - x_2|} \tag{5.1}$$

to compensate for the longer traversal of rays deviating from the principal direction.

5.1.3 A Simple Method

Köhler, Turbell, and Grass (2000) noted that the problem of calculating line-integrals can be separated into the two steps:

1. Construction of a continuous volume by interpolation from the discrete data
2. Line-integration in the continuous volume

A simple algorithm is obtained if the interpolation is chosen to be tri-linear and the integration through the continuous volume is approximated by summing values at equidistant points along the ray. See Figure 5.1(c).

The step width h is a free parameter that can be used to trade off between image quality and computation time. We introduce the quantity

$$N = \frac{\Delta x}{h} \tag{5.2}$$

A value of $N = 1$ corresponds to a sampling distance equal to the voxel sampling distance. The quantity N is therefore reffered to as an oversampling factor.

5.1.4 Köhler's Method

The Simpson rule of integration (Råde and Westergren 1990)

$$\int_a^b f(l)\, dl \approx \frac{b-a}{6}(f(a) + 4f(\frac{a+b}{2}) + f(b)) \tag{5.3}$$

can be used to numerically approximate the integral of a function given the function values at the integration borders and at the centre of the integration interval. For functions which are polynomials of third order the Simpson rule can be shown to be exact.

Let us define a *cell* as a box of sides Δx, Δy, and Δz with sampling points at its corners. The cells can be seen as voxels shifted half a sampling distance. Köhler et al. (2000) showed that tri-linear interpolation in step 1 above results in a volume where the density along a ray varies as a polynomial of third order within each

cell. It is therefore possible to calculate the line-integral in step 2 above analytically within each cell using the Simpson rule of integration.

The resulting method is illustrated in Figure 5.1(d) and consists of the following steps:

Algorithm 5.1 *Köhler's method of line-integration*

1: **for** each cell intersected by the ray **do**
2: calculate the function value at the two intersections of the cell wall using bi-linear interpolation
3: calculate the function value at the point halfway between the two intersection points above using tri-linear interpolation
4: combine the three values using Simpson's rule (5.3)
5: accumulate the result
6: **end for**

The values obtained by bi-linear interpolation at the wall intersections can be reused for the neighbouring cells. The free parameter h appearing in the simple approach is not used in the Köhler method.

5.2 Experimental results

We have calculated forward projections through the voxelized head phantom using the simple approach and Köhler's method. Figure 5.2(a) shows the root mean square difference between the two methods for different oversampling factors. A high oversampling factor is clearly needed in the simple approach to obtain the accuracy of Köhler's method. Figure 5.2(b) shows that the simple approach requires substantially more computation time for such a high oversampling factor.

In a second experiment we used an analytically described phantom with known projection values. The phantom was discretized as input to the algorithms. The results could then be compared with the ideal analytical values.

In order to avoid most of the aliasing a phantom such as a solid box or ellipsoid would result in we have chosen a spherically symmetric Kaiser-Bessel window as phantom. This window has only small frequency components above the Nyquist frequency related to our sampling distance Δx. It is defined as

$$f(x,y,z) = \frac{I_0(\alpha\sqrt{1-\frac{x^2+y^2+z^2}{a^2}})}{I_0(\alpha)} \tag{5.4}$$

where I_0 is the modified Bessel function of order 0. The free parameters a and α have been chosen as $a = N_x/2 = 4$ and $\alpha = \pi a$. The phantom was sampled at $(N_x \cdot M)^3 = 512M^3$ voxels of side $1/M$, where M is a variable oversampling factor.

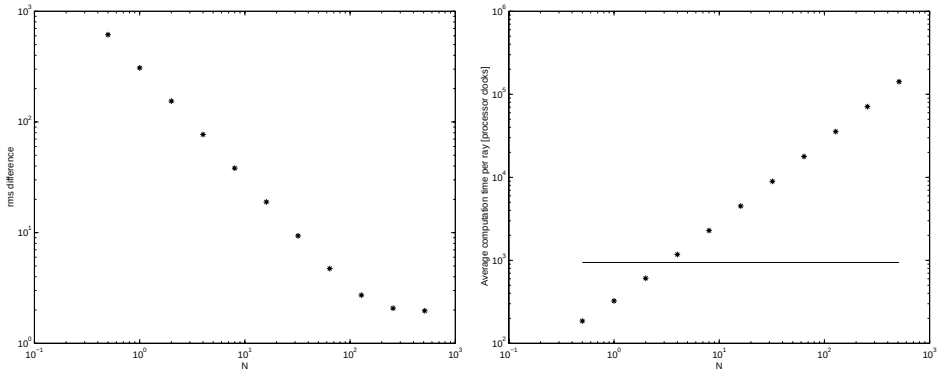

(a) Root mean square difference in arbitrary units between the simple approach and Köler's method. as a function of the oversampling N used in the simple approach.

(b) Average time needed by the simple approach as a function of the oversampling N. The line indicates the time needed using Köhler's approach.

Figure 5.2 *Comparisons between the simple approach and Köhler's method.*

Lewitt (1990) showed that the projection of a Kaiser-Bessel window only depends on the distance d between the ray and the window centre as

$$p(d) = \frac{2a}{\alpha I_0(\alpha)} \sinh\left(\alpha\sqrt{1-\frac{d^2}{a^2}}\right) \tag{5.5}$$

The root mean square of the difference between these ideal projection values and the calculated ones are plotted in Figure 5.3 as a function of the oversampling factor M. The Siddon method is clearly inferior to the methods of Joseph and Köhler that perform similarly.

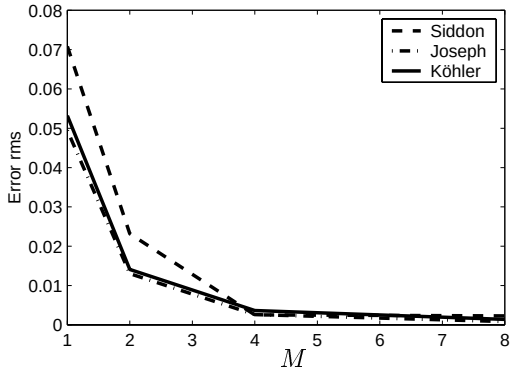

Figure 5.3 *Root mean square error of the projection values for three different forward projection methods as a function of the oversampling rate M.*

5.3 Discussion

At first sight, it might be surprising to see that the method of Joseph performs as good as the method of Köhler. We will now present an non-formal explanation.

The Siddon method can easily be expressed in the two steps mentioned above. The first step is an interpolation with the box function shown in Figure 5.4(a). The resulting volume is constant within each voxel. The weighting with the length of intersection clearly evaluates the line-integral through this volume analytically correct.

The Joseph method can also be expressed in the two steps. The interpolation should then be seen as being performed with a *sheared* tri-linear kernel as shown in Figure 5.4(b). The kernel axis parallel to the principal direction of the ray is sheared to be parallel with the ray. The other two kernel axes are kept unchanged. When the sheared axis of the kernel is parallel to the ray it is clear that an analytical integral through the kernel is identical to the bi-linear interpolation and compensation factor (5.1) in Joseph's method. Any smoothing in the direction of the ray is eliminated by the integration.

The only difference between the Joseph and Köhler methods is hence that the interpolation kernel in the Joseph method is a skewed version of the Köhler kernel in Figure 5.4(c). This should not have dramatic effects on the obtained quality. It is not obvious which kernel is optimal.

Figure 5.4(d) shows a rotated tri-linear kernel which could be considered as an alternative. However, the sum of the kernel values at the sample points not will be constant over the volume. It is therefore hard to formulate a practical algorithm for this kernel.

The four presented methods are all ray-driven. Alternative methods also exist. Lewitt (1992) has proposed the use of spherically symmetric interpolation kernels, also known as blobs. Mueller, Yagel, and Wheller (1999) investigate voxel driven approaches where a projection, a *footprint*, of each voxel is accumulated, *splatted*, onto the detector.

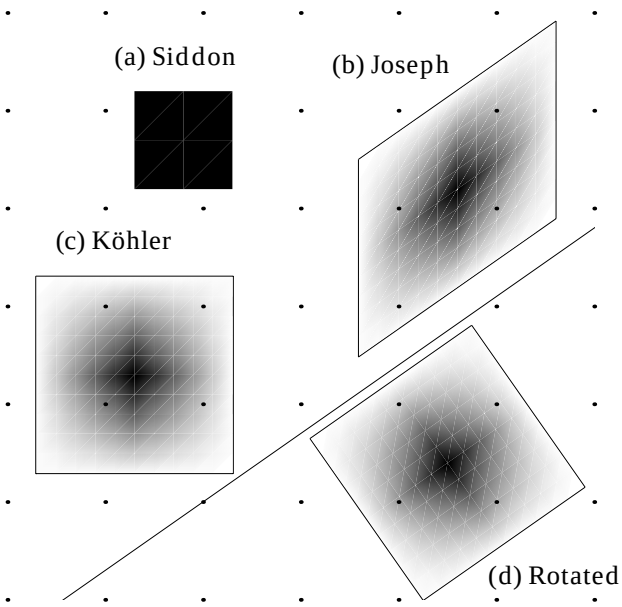

Figure 5.4 *Four interpolation kernels as seen along one axis. The line indicates the ray along which the integration is performed.*